

X-rays from the First Massive Black Holes

W.N. Brandt¹, C. Vignali², B.D. Lehmer¹, L.A. Lopez¹, D.P. Schneider¹, and I.V. Strateva¹

¹ Department of Astronomy & Astrophysics, The Pennsylvania State University, 525 Davey Lab, University Park, PA 16802, USA

² Dipartimento di Astronomia, Università degli Studi di Bologna, Via Ranzani 1, 40127 Bologna, Italy

Abstract. We briefly review some recent results from *Chandra* and *XMM-Newton* studies of the highest redshift ($z > 4$) active galactic nuclei (AGNs). Specific topics covered include radio-quiet quasars, radio-loud quasars, moderate-luminosity AGNs in X-ray surveys, and future prospects. No significant changes in AGN X-ray emission properties have yet been found at high redshift, indicating that the small-scale X-ray emission regions of AGNs are insensitive to the dramatic changes on larger scales that occur from $z \approx 0$ –6. X-ray observations are also constraining the environments of high-redshift AGNs, relevant emission processes, and high-redshift AGN demography.

1 Introduction

Understanding of the X-ray emission from the highest redshift ($z > 4$) active galactic nuclei (AGNs) has advanced rapidly over the past five years, due to the superb capabilities of *Chandra* and *XMM-Newton* combined with plentiful high-redshift discoveries by wide-field optical surveys. The number of X-ray detections at $z > 4$ has increased from 6 in 2000 to ≈ 100 today.

Are the first massive black holes feeding and growing in the same way as local ones? X-ray observations can address this question effectively, as they probe the immediate vicinity of the black hole where changes in the accretion mode should be most apparent. For example, high-redshift AGNs might typically have different values of $\dot{M}/\dot{M}_{\text{Edd}}$, given that they reside in young, forming galaxies that differ greatly from the majority of those in the local universe. Galactic black holes and local AGNs both show strong X-ray spectral changes with $\dot{M}/\dot{M}_{\text{Edd}}$ that should be detectable at high redshift (e.g., Brandt 1999; McClintock & Remillard 2004). X-ray observations can also constrain the environments of high-redshift AGNs (e.g., via X-ray absorption studies), relevant emission processes (e.g., in AGN jets), and high-redshift AGN demography.

We have been addressing the issues above using a combination of snapshot *Chandra* observations, spectroscopic *XMM-Newton* observations, X-ray survey data, and archival X-ray data. Below we will briefly review some of our results and will discuss some future prospects. We adopt $H_0 = 70 \text{ km s}^{-1} \text{ Mpc}^{-1}$, $\Omega_M = 0.3$, and $\Omega_A = 0.7$ throughout.

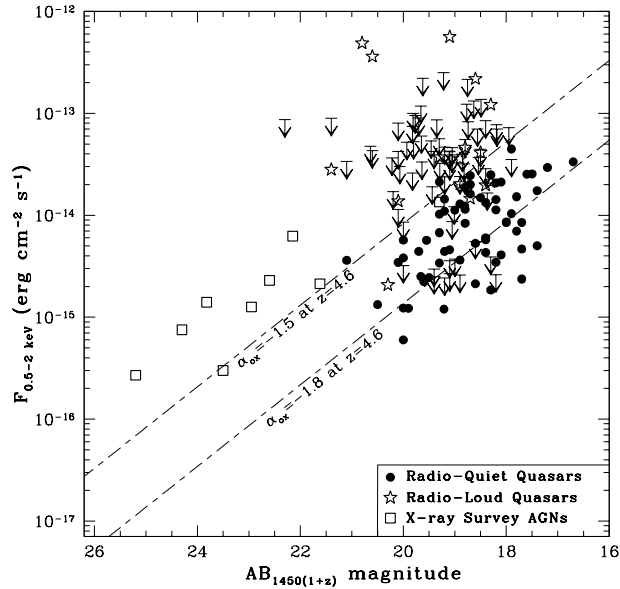


Fig. 1. Observed-frame, Galactic absorption-corrected 0.5–2 keV flux versus $AB_{1450(1+z)}$ magnitude for $z > 4$ AGNs. Object types are as shown in the legend; downward-pointing arrows indicate X-ray upper limits. The slanted lines show $\alpha_{ox} = -1.5$ and $\alpha_{ox} = -1.8$ loci at a fiducial redshift of $z = 4.6$. Adapted from Vignali et al. (2005).

2 High-Redshift Radio-Quiet Quasars

Most of the $z > 4$ AGNs with X-ray detections are luminous ($M_B < -26$) radio-quiet quasars (RQQs) that have been discovered in wide-field optical surveys and targeted with snapshot (4–12 ks) *Chandra* observations. For example, we have been targeting the most luminous RQQs ($M_B \approx -27$ to -29.5) from the Palomar Digital Sky Survey (DPOSS) and the Automatic Plate Measuring facility survey (APM) as well as some of the highest redshift RQQs ($z > 4.8$) from the Sloan Digital Sky Survey (SDSS).

Figure 1 shows the X-ray and optical fluxes for $z > 4$ AGNs with sensitive X-ray observations. As expected, the X-ray and optical fluxes for the RQQs are generally correlated, but there is significant scatter in this relation (see Vignali et al. 2003ac, 2005 for details). Even the optically brightest RQQs at $z > 4$ have relatively low 0.5–2 keV fluxes of a few $\times 10^{-14}$ $\text{erg cm}^{-2} \text{s}^{-1}$, so X-ray spectroscopy of these objects is challenging. Nevertheless, there has been respectable progress constraining the basic X-ray spectral properties of $z > 4$ RQQs using joint X-ray spectral fitting (Vignali et al. 2003ac, 2005) and single-object spectroscopy (Ferrero & Brinkmann 2003; Farrah et al. 2004; Grupe et al. 2004;

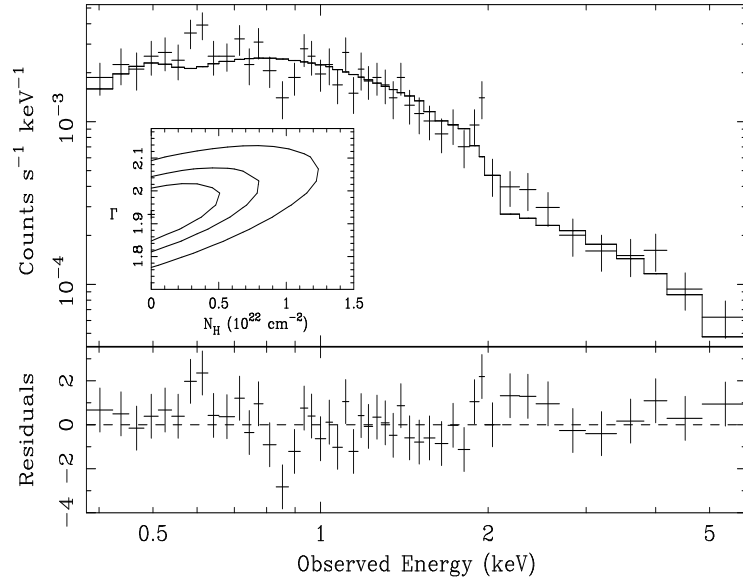


Fig. 2. Stacked *Chandra* spectrum constructed from 48 RQQs at $z = 3.99\text{--}6.28$. The spectrum has ≈ 870 source counts and an effective exposure time of 244 ks. The spectrum has been fit with a power-law model including Galactic absorption, and data-to-model residuals (in units of σ) are shown in the lower panel. The fit is statistically acceptable. The inset shows the 68, 90, and 99% confidence regions for the power-law photon index and intrinsic column density derived from joint spectral fitting with the Cash (1979) statistic. Adapted from Vignali et al. (2005).

Schwartz & Virani 2004). Figure 2, for example, shows the results from joint X-ray spectral fitting of 48 RQQs from $z = 3.99\text{--}6.28$ (with a median redshift of 4.43) using the Cash (1979) statistic (Vignali et al. 2005). This joint-fitting approach provides a stable estimate of average 2–40 keV rest-frame spectral properties. The spectrum is well fit by a power-law model with $\Gamma = 1.93^{+0.10}_{-0.09}$ and Galactic absorption; any widespread intrinsic absorption by neutral material has $N_{\text{H}} \lesssim 5 \times 10^{21} \text{ cm}^{-2}$. No iron K line emission or Compton reflection is detected, although the statistical constraints on such spectral components are not yet particularly meaningful.

Figure 3 summarizes the current X-ray spectral results on high-redshift RQQs, comparing their power-law photon indices to those of RQQs at lower redshift. There is significant intrinsic scatter in the photon indices at all redshifts. This scatter is believed to be due to object-to-object variations in the temperature and optical depth of the accretion-disk corona, likely arising from variations in $\dot{M}/\dot{M}_{\text{Edd}}$ (see Section 1). However, there is no detectable systematic change in the photon-index distribution at high redshift. On average, the accretion-disk coronae of high-redshift and low-redshift RQQs appear to have similar properties.

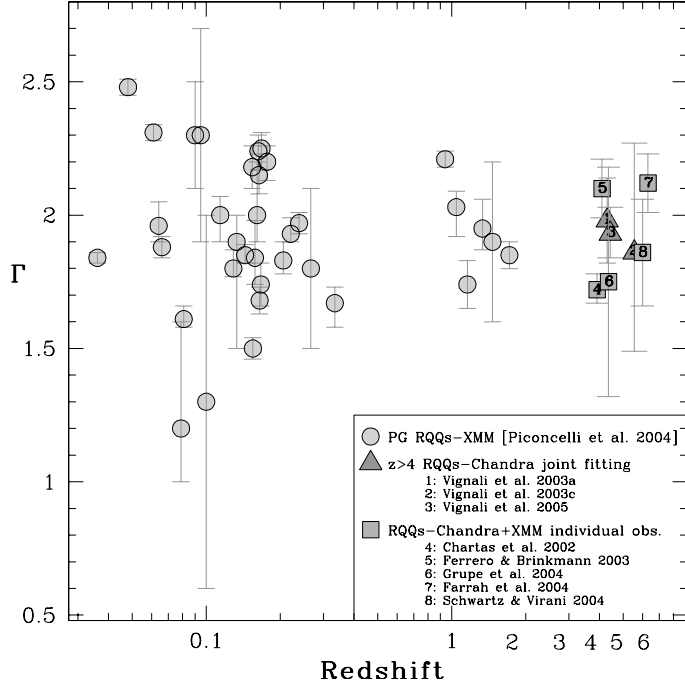


Fig. 3. Hard X-ray photon index versus redshift. The circles at $z < 2$ indicate RQQs from the Bright Quasar Survey (PG) analyzed by Piconcelli et al. (2004). At higher redshift, the data points have been derived from both joint spectral fitting (triangles) and single-object spectroscopy (squares); the data points are numbered with corresponding citations given in the figure legend.

In addition to measuring X-ray spectral properties, it is also informative to investigate relations between X-ray and longer wavelength emission. Any changes in accretion mode over cosmic time might lead to changes in the fraction of total power emitted as X-rays. Investigations of this type have been performed since the 1980's (e.g., Avni & Tananbaum 1986), often utilizing α_{ox} , which is defined as the point-to-point spectral slope between 2500 Å and 2 keV in the rest frame. Studies of the dependence of α_{ox} upon redshift and luminosity are challenging for several reasons: (1) broad ranges of sample redshift and luminosity are required to break statistical degeneracies between these two quantities, since they are correlated in flux-limited AGN samples, (2) a high fraction of X-ray detections is required to minimize statistical problems inherent in AGN samples with censoring, (3) absorbed AGNs, such as broad absorption line (BAL) quasars, need to be excluded when possible and controlled for when not, (4) radio-loud AGNs, which have an additional jet-linked X-ray emission component, need to be excluded, and (5) high-quality photometry/spectroscopy in the optical/UV,

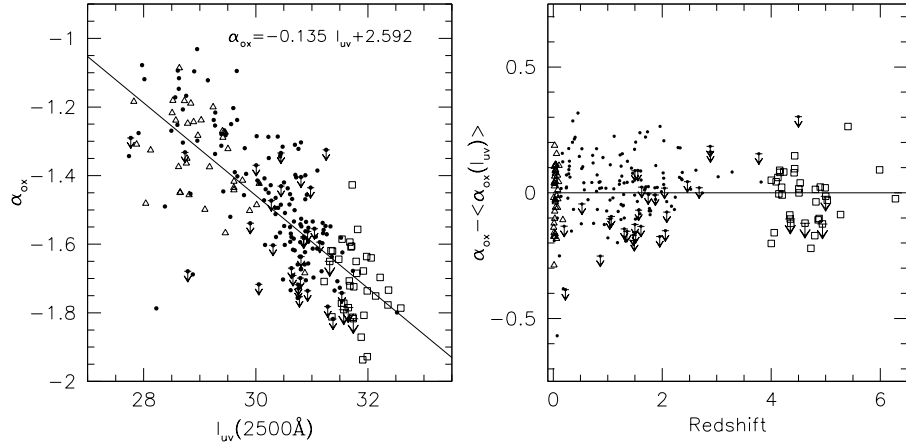


Fig. 4. The left panel shows α_{ox} versus 2500 \AA luminosity density for optically selected, radio-quiet AGNs: Seyfert 1 galaxies from Walter & Fink (1993; open triangles), SDSS AGNs in medium-depth *ROSAT* observations (filled circles), and $z > 4$ RQQs from Vignali et al. (2003c; open squares). Large negative values of α_{ox} correspond to relatively weak X-ray emission, and downward-pointing arrows indicate X-ray upper limits. The best fit to the data is also shown. The right panel shows α_{ox} residuals versus redshift after removing the best-fit luminosity dependence of α_{ox} . Note that no systematic trends remain. Adapted from Strateva et al. (2005).

allowing mitigation of host-galaxy contamination, is required. We are currently completing the most detailed study to date of the dependence of α_{ox} upon redshift and luminosity, taking into account the issues above (Strateva et al. 2005; also see Vignali, Brandt, & Schneider 2003b). We are predominantly utilizing a sample of 156 SDSS RQQs lying serendipitously in medium-depth *ROSAT* observations. Our partial correlation analyses find a highly significant (up to 10.7σ) anti-correlation between α_{ox} and 2500 \AA luminosity density when controlling for any redshift dependence (see Figure 4). In contrast, no significant correlation between α_{ox} and redshift is found when controlling for the 2500 \AA luminosity-density dependence. Qualitatively, our results are consistent with much, but not all, of the earlier work on this topic. Quantitatively, our results are more robust and have much better control of statistical and systematic errors than previous studies.

In summary, the typical RQQ (of a given luminosity) does not change its basic X-ray spectral shape or optical/UV-to-X-ray flux ratio over most of cosmic history. It appears that the small-scale X-ray emitting regions of RQQs are insensitive to the dramatic changes on larger scales that occur from $z \approx 0$ –6. The data are consistent with the idea that high-redshift RQQs are feeding and growing in basically the same way as local ones.

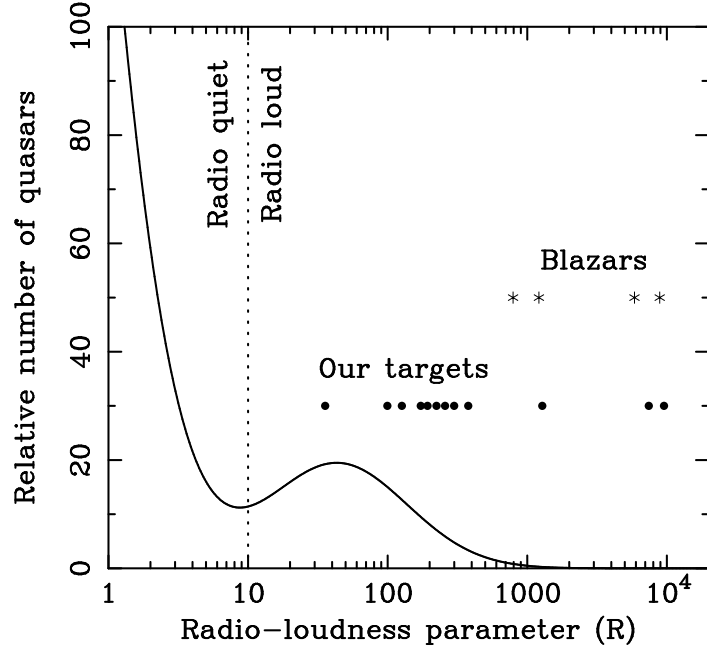


Fig. 5. The solid curve shows the relative number of quasars versus radio-loudness parameter (R) from Ivezić et al. (2002), and the dotted vertical line shows the standard R separation between RQQs and RLQs. Circles denote the R values for the RLQs we have been studying, and stars denote those for the four $z > 4$ blazars with X-ray spectra (the y -axis locations for these data points are arbitrary).

3 High-Redshift Radio-Loud Quasars

Until recently there were only a few $z > 4$ radio-loud quasars (RLQs) with sensitive X-ray observations. Most of these were highly radio-loud “blazars” with $R \approx 1000$ –10,000; here R is the standard radio-loudness parameter, defined as $R = f_{5 \text{ GHz}}/f_{4400 \text{ \AA}}$ (in the rest frame). While these blazars are not representative of the quasar population, or even the RLQ population, as a whole (see Figure 5), they have been intensively targeted for X-ray observations due to their relatively high X-ray fluxes (note the data points in Figure 1 with 0.5–2 keV fluxes of a few $\times 10^{-13} \text{ erg cm}^{-2} \text{ s}^{-1}$). Two of the four $z > 4$ blazars with X-ray spectra show evidence for substantial X-ray absorption (e.g., Worsley et al. 2004ab), a result that is broadly consistent with earlier findings that the fraction of RLQs with X-ray absorption rises with redshift (e.g., Cappi et al. 1997; Elvis et al. 1998; Fiore et al. 1998; Reeves & Turner 2000). The observed X-ray absorbing gas is thought to be associated with the RLQs’ environments, but its precise nature is unclear: it may be circumnuclear, located in the host galaxy, or entrained by the radio jets.

We have recently performed 4–8 ks *Chandra* snapshots to determine the basic X-ray properties of nine flat-spectrum RLQs with $R \approx 30$ –400 and $z = 4.0$ –4.8 (Bassett et al. 2004; Lopez et al. 2005). These lie much closer than the blazars to the peak of the R distribution for RLQs, and they are thus more representative of the high-redshift RLQ population (see Figure 5). We have also observed three recently discovered blazars with $R \approx 1300$ –9600 and $z = 3.5$ –4.6 to enlarge the sample of these objects with X-ray data. All 12 of our targets are clearly detected, and we have performed joint X-ray spectral fitting and α_{ox} analyses analogous to those described for RQQs in §2. As expected from similar RLQs at low redshift, the X-ray emission from our targets usually appears to have a large contribution from a jet-linked spectral component, probably synchrotron self-Compton emission arising on sub-parsec scales. The degree of X-ray enhancement provided by this component (relative to RQQs), as well as its X-ray spectral shape, appear consistent at high and low redshift. Our analyses of X-ray absorption via joint spectral fitting are ongoing, but they are challenging due to instrumental issues and limited photon statistics. Some X-ray absorption may be present with typical column densities of a few $\times 10^{22}$ cm $^{-2}$. *XMM-Newton* spectroscopy of several of these objects is needed to establish if X-ray absorption is common among typical flat-spectrum RLQs at high redshift, or if it is instead confined to the minority of RLQs with $R \gtrsim 1000$.

Our *Chandra* observations also provide useful constraints on kpc-scale X-ray jet emission from these RLQs; the on-axis angular resolution of *Chandra* at $z = 4$ corresponds to ≈ 4 kpc. One leading model for X-ray jet emission invokes highly relativistic bulk motions on kpc scales, thereby allowing electrons/positrons in the jet to Compton upscatter photons from the Cosmic Microwave Background (CMB) into the X-ray band (e.g., Tavecchio et al. 2000; Celotti, Ghisellini, & Chiaberge 2001). In this model, jets should remain X-ray bright at high redshift owing to the $(1+z)^4$ increase in CMB energy density which compensates for the usual $(1+z)^{-4}$ decrease of surface brightness (Schwartz 2002; also see, e.g., Rees & Setti 1968). In fact, if this model is correct, $z \gtrsim 4$ X-ray jets are often expected to outshine their X-ray cores (which dim with luminosity distance squared). We have looked for such X-ray luminous jets in our RLQ *Chandra* observations, and they are not detected. Any spatially resolvable X-ray jets must be ≈ 5 –10 times fainter than their X-ray cores.¹ In some cases jets might be unresolvable due to an almost perfectly “pole-on” orientation, but such an orientation is unlikely for all our RLQs (α_{ox} analyses also constrain this possibility). One plausible explanation for our nondetections is that most of the X-rays from RLQ jets are made via a process other than CMB Compton upscattering, such as synchrotron radiation by multiple electron populations (e.g., Atoyan & Dermer

¹ An X-ray jet has been detected from the $z = 4.30$ blazar GB 1508+5714 (Siemiginowska et al. 2003; Yuan et al. 2003). In this case, however, the jet-to-core X-ray flux ratio is $\approx 3\%$, substantially less than the $\approx 100\%$ discussed by Schwartz (2002). Additionally, the putative X-ray jet from the $z = 4.01$ blazar GB 1713+2148 (Schwartz 2004) is not confirmed in a pointed *Chandra* observation (D.A. Schwartz 2004, pers. comm.).

Table 1. Moderate-luminosity $z > 4$ AGNs found in X-ray surveys

| AGN name | Redshift | Rest-frame $\log(L_{2-10})$ | Representative reference |
|-----------------------------|----------|-----------------------------|--------------------------|
| CXOCY J033716.7 – 050153 | 4.61 | 44.54 | Treister et al. (2004) |
| CLASXS J103414.33+572227 | 5.40 | 44.44 | Steffen et al. (2004) |
| RX J1052 + 5719 | 4.45 | 44.72 | Schneider et al. (1998) |
| CXOMP J105655.1 – 034322 | 4.05 | 44.92 | Silverman et al. (2005) |
| CXO HDFN J123647.9 + 620941 | 5.19 | 44.00 | Vignali et al. (2002) |
| CXO HDFN J123719.0 + 621025 | 4.14 | 43.72 | Vignali et al. (2002) |
| CXOCY J125304.0 – 090737 | 4.18 | 44.39 | Castander et al. (2003) |
| CXOMP J213945.0 – 234655 | 4.93 | 44.79 | Silverman et al. (2002) |

The third column above is the rest-frame 2–10 keV luminosity (in erg s^{-1}), computed using a power-law photon index of $\Gamma = 2$. We have only included AGNs in this table with $\log(L_{2-10}) < 45$. A few higher luminosity AGNs have also been found in X-ray surveys, such as RX J1028.6–0844 (Zickgraf et al. 1997) and RX J1759.4+6638 (Henry et al. 1994).

2004; Stawarz et al. 2004). Alternatively, RLQ jets may often be “frustrated” at high redshift by their environments and thus only rarely achieve large angular sizes; this possibility can be tested with improved high-resolution radio imaging of $z > 4$ RLQs.

4 X-ray Survey Constraints on Moderate-Luminosity Active Galactic Nuclei at High Redshift

The analyses above engender confidence that X-ray selection should remain effective at finding AGNs at the highest redshifts, and the deepest current surveys with *Chandra* and *XMM-Newton* (e.g., Brandt & Hasinger 2005) have sufficient sensitivity to detect $z > 4$ AGNs that are ≈ 10 –30 times less luminous than the quasars found in wide-field optical surveys (see Figure 1). For example, AGNs similar to Seyfert galaxies in the local universe, with X-ray luminosities of $\gtrsim 5 \times 10^{43} \text{ erg s}^{-1}$, should be detectable to $z \approx 10$ in the 2 Ms *Chandra* Deep Field-North (CDF-N; Alexander et al. 2003) observation. Such moderate-luminosity AGNs are much more numerous and thus more representative of the AGN population than the luminous quasars from wide-field optical surveys. Furthermore, X-ray surveys suffer from progressively less absorption bias as higher redshifts are surveyed (penetrating ≈ 2 –40 keV rest-frame X-rays are sampled at $z > 4$), whereas optical surveys sample rest-frame ultraviolet light which can be absorbed by dust.

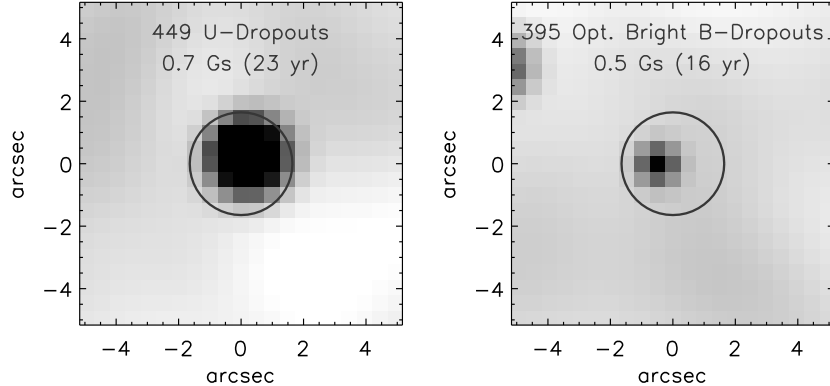


Fig. 6. Stacked images of Lyman break galaxies from the Great Observatories Origins Deep Survey (GOODS) in the 0.5–2 keV band. The left panel shows the stacking results for 449 U -dropouts with a typical redshift of $z = 3.0$ (7.1σ detection), and the right panel shows those for 395 optically bright B -dropouts with a typical redshift of $z = 3.8$ (3.2σ detection). The effective exposure times for the left and right panels are 23 and 16 yr, respectively. Adapted from Lehmer et al. (2005).

Moderate-luminosity X-ray detected AGNs at $z = 4$ –6.5 are expected to have I -band magnitudes of ≈ 23 –27; optical spectroscopy of these objects is thus challenging. Nevertheless, significant constraints on sky density have been set via intensive follow-up studies with large optical telescopes and color selection (e.g., Alexander et al. 2001; Barger et al. 2003; Cristiani et al. 2004; Koekemoer et al. 2004; Wang et al. 2004b). The sky density of $z > 4$ AGNs is ≈ 30 –150 deg^{-2} at a 0.5–2 keV flux limit of $\approx 10^{-16} \text{ erg cm}^{-2} \text{ s}^{-1}$; for comparison, the sky density of $z = 4$ –5.4 SDSS quasars is $\approx 0.12 \text{ deg}^{-2}$ at an i -magnitude limit of ≈ 20.2 (e.g., Schneider et al. 2003). While the constraints on the faint end of the AGN X-ray luminosity function at $z > 4$ have large statistical errors, the data are already sufficient to argue convincingly that the AGN contribution to reionization at $z \approx 6$ is small.

Table 1 lists the moderate-luminosity $z > 4$ AGNs found in X-ray surveys. The number of objects is small but is increasing fairly rapidly, as can be seen from the publication dates of the associated papers. With appropriate effort it should be possible to generate ≈ 50 moderate-luminosity $z > 4$ AGNs over the next ≈ 5 years, thereby defining in respectable detail the faint end of the luminosity function. Current X-ray spectral and α_{ox} analyses, albeit limited, suggest that the moderate-luminosity $z > 4$ AGNs found in X-ray surveys have similar basic emission properties to comparably luminous objects at low redshift (e.g., Vignali et al. 2002).

High-redshift AGN populations with even lower luminosities can be constrained with X-ray source-stacking analyses. These search for an average signal from a set of high-redshift sources whose individual members lie below the single-source X-ray detection limit. The most sensitive X-ray source-stacking analyses at $z \approx 4$ or higher have employed samples of ≈ 250 – 1700 Lyman break galaxies (e.g., Lehmer et al. 2005; B , V , and i dropouts) and ≈ 100 Ly α emitters (e.g., Wang et al. 2004a; at $z \approx 4.5$). Average X-ray detections have presently been obtained up to $z \approx 4$ (see Figure 6), while physically interesting upper limits are obtained at higher redshifts. The data are plausibly consistent with any X-ray emission from these objects arising from stellar processes (e.g., X-ray binaries and supernova remnants); X-ray emission from numerous, low-luminosity AGNs is not required. These average constraints at luminosities below those that can be probed by single-source analyses further limit the contribution that AGNs could have made to reionization at $z \approx 6$. A complementary average constraint, derived by considering the unresolved component of the 0.5–2 keV background, provides additional evidence that AGNs and lower mass black holes did not dominate reionization (Dijkstra, Haiman, & Loeb 2004).

5 Some Future Prospects

The work described above can be extended in several ways with *Chandra* and *XMM-Newton* observations:

1. The number of X-ray detections at $z > 5$ is still relatively small at present, and this can be increased substantially with appropriate *Chandra* snapshots of the highest redshift quasars.
2. Only the most basic X-ray properties of typical RLQs at $z > 4$ are now known. *XMM-Newton* spectroscopy should allow their X-ray continuum and absorption properties to be determined much better, and deeper *Chandra* imaging of some objects is needed to search for X-ray jets more sensitively (in conjunction with improved radio imaging). Steep-spectrum RLQs at $z > 4$ also need to be studied in the X-ray band.
3. Additional X-ray investigations of minority AGN populations at $z > 4$, such as weak emission-line quasars and BAL quasars, can provide insight into their nature.
4. X-ray studies of $z > 4$ AGNs selected at infrared, submillimeter, and millimeter wavelengths (or with remarkable properties at these wavelengths) can establish the relative importance of AGN vs. stellar processes in these objects and allow assessment of extinction biases.
5. The number of known moderate-luminosity AGNs at $z > 4$ should increase significantly over the next few years, as follow-up studies of the many ongoing X-ray surveys progress. Uniform searches for such AGNs are particularly important for setting reliable demographic constraints.
6. Deeper X-ray surveys than those to date (e.g., 5–10 Ms *Chandra* observations) would allow improved searches for highly obscured AGNs at $z > 4$.

7. X-ray stacking analyses can be improved as high-redshift source samples are enlarged and refined.

In the more distant future, *Constellation-X* and *XEUS* should allow X-ray spectroscopy down to 0.5–2 keV flux levels of $\approx 5 \times 10^{-16}$ and $\approx 5 \times 10^{-17}$ erg cm $^{-2}$ s $^{-1}$, respectively (see Figure 1). Precise X-ray measurements of continuum shape, absorption, iron K line emission, and Compton reflection should be possible for many $z > 4$ AGNs. Ultimately, a mission such as *Generation-X* should be able to survey the $z \approx 10$ –15 X-ray universe, searching for X-rays from proto-quasars and the ≈ 100 –300 M $_{\odot}$ black holes made by the deaths of the first stars.

Acknowledgments

We thank all of our collaborators on this work. We thank D.M. Alexander, L.C. Bassett, F.E. Bauer, C.C. Cheung, S. Heinz, D.A. Schwartz, and A.T. Steffen for helpful discussions. We acknowledge funding from NASA LTSA grant NAG5-13035 (WNB, DPS, IVS), NSF CAREER award AST-9983783 (WNB, BDL), *Chandra* and *XMM-Newton* grants (WNB, DPS), and MIUR COFIN grant 03-02-23 (CV).

References

1. D.M. Alexander, W.N. Brandt, A.E. Hornschemeier, et al.: AJ **122**, 2156 (2001)
2. D.M. Alexander, F.E. Bauer, W.N. Brandt, et al.: AJ **126**, 539 (2003)
3. A. Atoyan, C.D. Dermer: ApJ **613**, 151 (2004)
4. Y. Avni, H. Tananbaum: ApJ **305**, 83 (1986)
5. A.J. Barger, L.L. Cowie, P. Capak, et al.: ApJ **584** L61 (2003)
6. L.C. Bassett, W.N. Brandt, D.P. Schneider, C. Vignali, G. Chartas, G.P. Garmire: AJ **128**, 523 (2004)
7. W.N. Brandt: ‘Ultrasoft Narrow-Line Seyfert 1 Galaxies: An Extreme of the Seyfert Phenomenon’. In: *High Energy Processes in Accreting Black Holes*, ed. by J. Poutanen, R. Svensson (ASP, San Francisco 1999), pp. 166–177
8. W.N. Brandt, G. Hasinger: ARA&A, submitted (2005)
9. M. Cappi, M. Matsuoka, A. Comastri, et al.: ApJ **478**, 492 (1997)
10. W. Cash: ApJ **228**, 939 (1979)
11. F.J. Castander, E. Treister, T.J. Maccarone, et al.: AJ **125**, 1689 (2003)
12. A. Celotti, G. Ghisellini, M. Chiaberge: MNRAS **321**, L1 (2001)
13. G. Chartas, W.N. Brandt, S.C. Gallagher, G.P. Garmire: ApJ **579**, 169 (2002)
14. S. Cristiani, D.M. Alexander, F.E. Bauer, et al.: ApJ **600**, L119 (2004)
15. M. Dijkstra, Z. Haiman, A. Loeb: ApJ **613**, 646 (2004)
16. M. Elvis, F. Fiore, P. Giommi, P. Padovani: ApJ **492**, 91 (1998)
17. D. Farrah, R. Priddey, R. Wilman, M. Haehnelt, R. McMahon: ApJ **611**, L13 (2004)
18. E. Ferrero, W. Brinkmann: A&A **402**, 465 (2003)
19. F. Fiore, M. Elvis, P. Giommi, P. Padovani: ApJ **492**, 79 (1998)
20. D. Grupe, S. Mathur, B.J. Wilkes, M. Elvis: AJ **127**, 1 (2004)
21. J.P. Henry, I.M. Gioia, H. Boehringer, et al.: AJ **107**, 1270 (1994)

22. Z. Ivezić, G.T. Richards, P.B. Hall, et al.: 'Quasar Radio Dichotomy: Two Peaks, or not Two Peaks, that is the Question'. In: *AGN Physics with the Sloan Digital Sky Survey*, ed. by G.T. Richards, P.B. Hall (ASP, San Francisco 2004) pp. 347–350
23. A.M. Koekemoer, D.M. Alexander, F.E. Bauer, et al.: *ApJ* **600**, L123 (2004)
24. B.D. Lehmer, W.N. Brandt, D.M. Alexander, et al.: *AJ*, in press (2005; astro-ph/0409600)
25. L.A. Lopez, W.N. Brandt, D.P. Schneider, C. Vignali, G. Chartas, G.P. Garmire: *AJ*, in preparation (2005)
26. J.E. McClintock, R.A. Remillard: 'Black Hole Binaries'. In: *Compact Stellar X-ray Sources*, ed. by W.H.G. Lewin, M. van der Klis (Cambridge University Press, Cambridge 2004), in press (astro-ph/0306213)
27. E. Piconcelli, E. Jimenez-Bailón, M. Guainazzi, N. Schartel, P.M. Rodriguez-Pascual, M. Santos-Lleó: *A&A*, in press (2004; astro-ph/0411051)
28. M.J. Rees, G. Setti: *Nature* **219**, 127 (1968)
29. J.N. Reeves, M.J.L. Turner: *MNRAS* **316**, 234 (2000)
30. D.P. Schneider, M. Schmidt, G. Hasinger, et al.: *AJ* **115**, 1230 (1998)
31. D.P. Schneider, X. Fan, P.B. Hall, et al.: *AJ* **126**, 2579 (2003)
32. D.A. Schwartz: *ApJ* **569**, L23 (2002)
33. D.A. Schwartz, S.N. Virani: *ApJ* **615**, L21 (2004)
34. D.A. Schwartz: 'An X-ray View of Radio Sources'. In: *Radio Astronomy at 70: From Karl Jansky to Microjansky*, ed. by L. Gurvits, S. Frey, S. Rawlings (EDP Sciences, Les Ulis 2004), in press (astro-ph/0402303)
35. A. Siemiginowska, R.K. Smith, T.L. Aldcroft, D.A. Schwartz, F. Paerels, A.O. Petric: *ApJ* **598**, L15 (2003)
36. J.D. Silverman, P.J. Green, D.W. Kim, et al.: *ApJ* **569**, L1 (2002)
37. J.D. Silverman, P.J. Green, W.A. Barkhouse, et al.: *ApJ*, in press (2005; astro-ph/0409337)
38. L. Stawarz, M. Sikora, M. Ostrowski, M.C. Begelman: *ApJ* **608**, 95 (2004)
39. I.V. Strateva, W.N. Brandt, D.P. Schneider, D.G. Vanden Berk, C. Vignali: *AJ*, in preparation (2005)
40. A.T. Steffen, A.J. Barger, P. Capak, L.L. Cowie, R.F. Mushotzky, Y. Yang: *AJ* **128**, 1483 (2004)
41. F. Tavecchio, L. Maraschi, R.M. Sambruna, C.M. Urry: *ApJ* **544**, L23 (2000)
42. E. Treister, F.J. Castander, T.J. Maccarone, et al.: *ApJ* **603**, 36 (2004)
43. C. Vignali, F.E. Bauer, D.M. Alexander, et al.: *ApJ* **580**, L105 (2002)
44. C. Vignali, W.N. Brandt, D.P. Schneider, G.P. Garmire, S. Kaspi: *AJ* **124**, 418 (2003a)
45. C. Vignali, W.N. Brandt, D.P. Schneider: *AJ* **125**, 433 (2003b)
46. C. Vignali, W.N. Brandt, D.P. Schneider, et al.: *AJ* **125**, 2876 (2003c)
47. C. Vignali, W.N. Brandt, D.P. Schneider, S. Kaspi: *AJ*, submitted (2005)
48. J.X. Wang, J.E. Rhoads, S. Malhotra, et al.: *ApJ* **608**, L21 (2004a)
49. J.X. Wang, S. Malhotra, J.E. Rhoads, C.A. Norman: *ApJ* **612**, L109 (2004b)
50. M.A. Worsley, A.C. Fabian, A. Celotti, K. Iwasawa: *MNRAS* **350**, L67 (2004a)
51. M.A. Worsley, A.C. Fabian, A.K. Turner, A. Celotti, K. Iwasawa: *MNRAS* **350**, 207 (2004b)
52. W. Yuan, A.C. Fabian, A. Celotti, P.G. Jonker: *MNRAS* **346**, L7 (2003)
53. F.J. Zickgraf, W. Voges, J. Krautter, et al.: *A&A* **323**, L21 (1997)